CERAMIC

JOURNAL OF CERAMIC PROCESSING RESEARCH

Volume 24, Number 3, 2023

ISSN : 1229-9162 (Print)
ISSN : 2672-152X (Online)

JOURNAL OF CERAMIC PROCESSING RESEARCH

2023

Volume 24, Number 3

International Organization for Ceramic Processing

J O U R N A L O F

Ceramic Processing Research

Volume 24, Number 3, June 2023

CONTENTS

Research Articles

Journal of Ceramic Processing Research. Vol. 24, No. 3, pp. 471~477 (2023)
(Received 13 January 2023, Received in revised form 11 May 2023, Accepted 17 May 2023)
https://doi.org/10.36410/jcpr.2023.24.3.471

J O U R N A L O F
Ceramic Processing Research

Characterization of some natural materials with different morphologies and their mullitization in ceramic preparation

Nguyen Thi Thanh Thao[a,b,*] and Bui Hoang Bac[a,b]
[a]*Faculty of Geosciences and Geology Engineering, Hanoi University of Mining and Geology, Hanoi, Vietnam*
[b]*HiTech-CEAE Research Team, Hanoi University of Mining and Geology, Hanoi, Vietnam*

This study aimed to investigate the characteristics of three types of natural materials (KLC, KPT, and SSB) obtained from regular deposits in Vietnam and their mullitization at calcinated temperatures of 1000 °C, 1200 °C, and 1400 °C. The samples were characterized by X-ray diffraction (XRD), X-ray fluorescence analysis (XRF), thermal analysis (the thermogravimetry/ differential scanning calorimetry (TG/DSC)), and scanning electron microscope with energy-dispersive X-ray spectroscopy (SEM-EDS). The results indicated that kaolinite, halloysite, and sericite are the dominant minerals in the KLC, KPT, and SSB samples, with particle sizes under 2 μm. These minerals' morphology was typical, with pseudo-hexagonal and stratified kaolinite, tubular halloysite, and thin platy sericite. The samples' chemical compositions are mainly SiO_2 and Al_2O_3, followed by (K_2O+Na_2O), TiO_2, and total iron content. Thermal analysis shows that the metakaolin phase is formed at different temperatures for the halloysite and kaolinite samples, as indicated by endothermic peaks at 411 °C for KPT and 436 °C for KLC. The quartz phase transition is also detected at different temperatures for the samples, with low-to-high temperature endothermic peaks at 559 °C (KPT), 569 °C (KLC), and 575 °C (SSB). The mullitization process is observed to start at temperatures above 1000 °C and is critical at around 1400 °C, with well-crystal mullites appearing. The mineral composition and morphology of the starting materials influence the size of the mullite crystals. SSB has larger mullite crystals than KLC and KPT at a sintering temperature of 1400 °C. It suggests that mineral composition, mineral morphology, and particle size of starting materials can also be essential factors influencing to mullitization process and ceramic products.

Keywords: Pseudo-hexagonal kaolinite, Tabular halloysite, Platy sericite, Mullite, Thermal analysis, Ceramics.

Introduction

Mullite, with a general chemical formation of $3Al_2O_3{\cdot}2SiO_2$, is an important ceramic material with attractive properties such as high melting point, low thermal conductivity and expansion, good creep resistance, corrosion stability, and excellent chemical stability at high temperatures [1-3]. Mullite can produce ceramics with better strength and toughness than other popular ceramic products [4].

Mullites have diverse applications in many fields, leading to numerous studies being conducted to prepare them from various sources, such as industrial waste and natural minerals [5-7]. A few studies can be mentioned here. Tan [8] utilized coal fly ash with primary components Al_2O_3 and SiO_2 (Al_2O_3/SiO_2=0.32, molar ratio) and aluminum sulfate in a sodium sulfate flux to synthesize mullite whiskers with a diameter of 0.06-0.3 μm at a calcination temperature of 1000 °C. Tong and his colleagues synthesized a porous mullite ceramic support using fly ash, loess, bauxite, calcium carbonate, and polyvinyl alcohol. It showed that the support had a porosity of 46.3% and a flexural strength of 77.7 MPa when sintered at 1200 °C with 5% calcium carbonate content [9]. In addition to industrial waste, natural minerals, especially aluminosilicate minerals, are used a lot in making mullite with different properties. Silva et al. produced porous mullite blocks using kaolin and alumina waste compositions. The results show that the size of the mullite needles was calculated to have diameters smaller than 400 nm [10]. Yuan et al. performed a proposal for the preparation of porous mullite ceramics containing needle-liked whiskers from a powder mixture of kaolinite, $Al(OH)_3$, and starch with NH_4F as an additive [11]. In this study, mullite is the only crystalline phase detected at 1400 °C with a dense network of rod-shaped and elongated needle-like crystals. From some of the studies above, it is evident that mullitization and the structure of mullite crystals depend mainly on the initial materials used (including their chemical and mineral composition, particle size, and so on) as well as the synthesis method. Therefore, it is essential to fully evaluate the starting materials' characteristics to obtain the necessary information for producing effective mullite ceramics.

In this study, X-ray diffraction (XRD), X-ray fluorescence analysis (XRF), thermal analysis (TG/ DSC), and scanning electron microscope with energy-

*Corresponding author:
Tel : +82 43 838 4973
Fax: +82 43 838 9633
E-mail: nguyenthithanhthao@humg.edu.vn

dispersive X-ray spectroscopy (SEM-EDS) were utilized to study three types of natural materials (KLC, KPT, and SSB) with distinct morphologies sourced from standard deposits in Vietnam. The materials were also subjected to calcinate at temperatures of 1000 °C, 1200 °C, and 1400 °C to investigate their mullitization.

Materials and Methods

Materials

Three natural materials were obtained from different mines in Vietnam, including one sample of kaolin from Son Man mine, Lao Cai province (KLC), one sample of kaolin from Lang Dong mine, Phu Tho province (KPT), and sericite from Son Binh mine, Ha, Tinh province (SSB). The Son Binh sericite develops in the Lower Triassic Dong Trau sub-formation with compositions of rhyolite rocks, rhyolitic tuff, tuffaceous sandstone, tuffaceous siltstone, and quartz porphyry. Sericite is formed by transforming potassium feldspar and plagioclase at medium-low temperatures [12-14]. Kaolin of Son Man mine was created by weathering pegmatites belonging to phase 2 of the Neoproterozoic - Early Cambrian Xom Giau complex. The pegmatites are composed mainly of feldspar, quartz, and little mica and are distributed in the Ngoi Chi formation. Tabular halloysite minerals in the Lang Dong deposit have been found in the weathered pegmatites of the Late Paleozoic Tan Phuong granite complex. They are widely distributed in the Proterozoic metamorphic Thach Khoan formation [15]. Typical types of non-metallic mineral deposits have been exploited to provide raw natural materials for various applications in Vietnam.

Preparation

The bulk samples (KLC, KPT, and SSB) were first dissolved using deionized water and filtered through a 63-micrometer sieve. Particles under the 63-micrometer sieve (raw samples) were dried and used for further experiments and analyses. The < 2 mm clay sample fraction was obtained using decantation to determine clay minerals. The size fractions < 2 mm were mounted as oriented aggregate mounts. Those can be used for other treatments, including air drying, glycolation with ethylene glycol, and heating to 350 °C.

Cylindrical pellets were prepared by uniaxial dry pressing the KLC, KPT, and SSB samples at 40 MPa and then were air-dried for 24 h at 60 ºC using an oven. After that, they were heated at 1000 ºC, 1200 ºC, and 1400 ºC with a heating rate of 5 $K.min^{-1}$, using an electric laboratory furnace (Nabertherm furnace). The samples were calcined for two hours for each chosen temperature and then slowly cooled to room temperature. The calcined KLC, KPT, and SSB samples at 1000 ºC, 1200 ºC, and 1400 ºC are named (KLC10, KPT10, SSB10), (KLC12, KPT12, SSB12), and (KLC14, KPT14, SSB14), respectively. Pieces of KLC14, KPT14, and SSB14 samples were put in 5% hydrofluoric acid (HF) vial for 20 minutes and then imaged using SEM.

Characterization

X-ray powder diffraction (XRD) patterns were measured using a D5005 Siemens model powder diffractometer with Cu-Kα radiation at 40 kV and 30 mA. All samples were scanned from 3 to 70° at a goniometer rate of $2\theta=2°min^{-1}$. Clay minerals were identified using the Joint Committee of Powder Diffraction Standards (JCPDS) software. X-ray fluorescence analysis (XRF, Philips X Unique2) determined the major-element chemical analysis on pressed powder samples. The morphological properties and chemical elements were examined using the scanning electron microscope (SEM-Quanta 450) with energy-dispersive X-ray spectroscopy (EDS). The sintering behaviors of the samples were evaluated by thermogravimetric analysis-differential scanning calorimetry (TG-DSC) from room temperature to 1000 °C at a heating rate of 10 °C/min in air.

Results and Discussion

Characterization of the natural materials

X-ray analysis

The X-ray diffraction (XRD) patterns of the natural materials (KLC, KPT, and SSB) under 2 μm size fractions in different experimental conditions (oriented at room temperature, ethylene glycol, and 350 °C) are presented in Fig. 1. The XRD patterns in Fig. 1a indicate that kaolinite is the predominant mineral in the KLC sample with typical peaks of 7.18 Å, 4.48 Å, and 3.58 Å. The weak basal reflections at 10.0 Å, 5.02 Å, and 3.35 Å present the existence of the muscovite mineral. The XRD peaks of the kaolinite and muscovite minerals did not shift under the experimental conditions of treating with ethylene glycol and heating at 350 °C. The broad XRD patterns of the KPT also show minerals of the kaolin group with the basal spacing at peaks of 10.0 Å, 7.18 Å, 4.43Å và 3.59 Å (Fig. 1b) [15]. The reflections at 10.0 Å and 7.42 Å indicate that 7Å halloysite and kaolinite coexist in the sample. The shift of the 10.0 Å to 10.5 Å positions under the condition of treatment with ethylene glycol chemical, also referred to as halloysite mineral in the sample [16]. The peak of 10 Å halloysite mineral was moved to the kaolinite mineral of 7.18 Å at a heating condition of 350 °C due to water loss in the halloysite layers. Although kaolinite and halloysite have similar chemical formulas, they show variations in their XRD peak patterns under different experimental conditions, possibly due to differences in their structures. Meanwhile, the minerals of sericite, chlorite, pyrophyllite, quartz, and feldspar in the SSB sample are pretty stable, and their XRD patterns do not change in the treatment of ethylene glycol and heating at 350 °C (Fig. 1c).

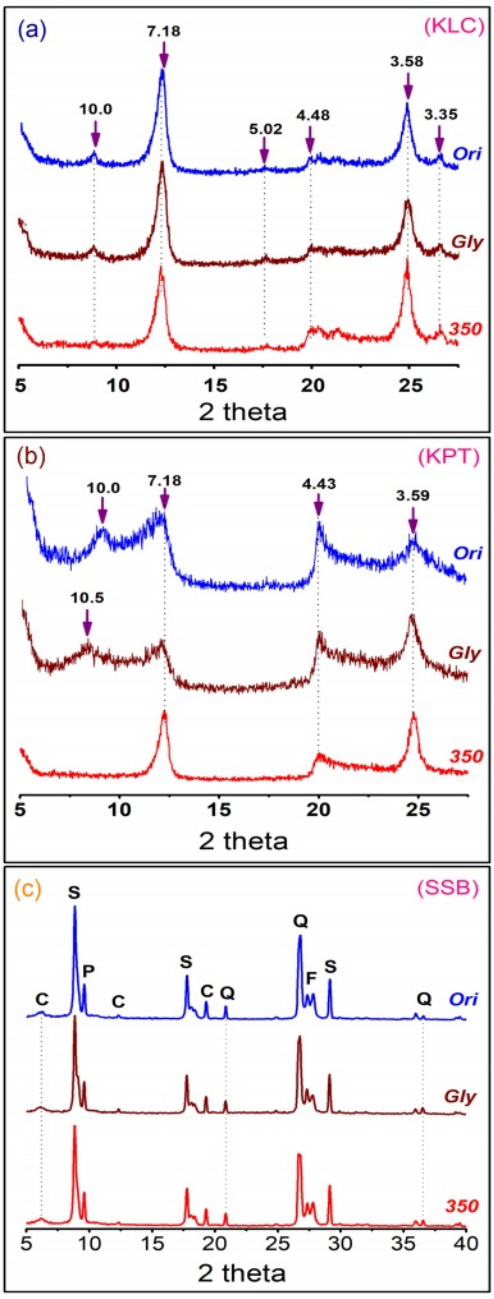

Fig. 1. XRD pattern of the sample of the size fraction < 2 mm in different experimental conditions (oriented aggregate at room temperature (*Ori*), ethylene glycol (*Gly*) and at 350 °C (*350*)). Note: (a). KLC sample, (b). KPT sample, (c). SSB sample, C - Chlorite, S - Sericite, P - Pyrophyllite, Q - Quartz, and F - Feldspar.

X-ray fluorescence analysis

The chemical composition of the natural materials was determined by XRF and presented in Table 1. The results show that silica and alumina are the common oxides (SiO_2 and Al_2O_3) with the highest percentage in the three samples. Minor amounts of other oxides are titanium oxide (TiO_2), total iron content (T.Fe), and alkaline elements (Na_2O+K_2O). SiO_2 content in the SSB sample (62.91%) is much higher than that in the KLC (43.08%) and KPT (48.50%) samples. It indicates that the SSB sample contains Si minerals, such as quartz, pyrophyllite, and feldspar. The loss on ignition (LOI) in the SSB sample (2.03%) is relatively small compared to that in KLC (12.68%) and KPT (13.15%) samples. The KLC and KPT samples are composed of significant amounts of physically combined water, chemically combined water, and volatile matter. Those are also consistent with the above results of XRD and SEM-EDS analysis.

Scanning electron microscopy and Energy dispersive analysis

The difference between the main minerals in the three natural materials is clearly shown in the scanning electron microscopy (SEM) images (Fig. 2). The pseudo-hexagonal and stratified structure of the kaolinite mineral was observed in the KLC sample (Fig. 2a). Meanwhile, tubular halloysite minerals predominated in the KPT sample (Fig. 2b). sericite, the predominant mineral in the SSB sample) with thin plates clearly shown in Fig. 2c. These results are similar to previously published results [15, 17]. Thus, it can be seen that each type of natural material contains a prominent mineral with different structural morphology, that is, halloysite ($Al_2Si_2O_5(OH)_4{\cdot}nH_2O$) or kaolinite ($Al_2Si_2O_5(OH)_4$) and sericite (K, Na, Ca) (Al, Fe, Mg)$_2$(Si, Al)$_4O_{10}(OH)_2$). This may have specific effects on mullite formation after high-temperature calcination.

Thermal analysis

The results of the thermogravimetry/differential scanning calorimetry (TG/DSC) of the KLC and KPT samples are shown in Fig. 3a, b. Fig 3c presents the SSB sample's thermogravimetry/differential thermal analysis (TG/DTA) [17]. The thermal curves in Fig. 3 show various reaction peaks (endothermic and exothermic processes) during heating. The endothermic reactions at

Table 1. Chemical compositions of the natural materials.

Natural materials	Chemical composition (%)						
	SiO_2	Al_2O_3	TiO_2	T.Fe[a]	K_2O	Na_2O	LOI[b]
KLC sample	43.08	35.05	0.11	1,00	2.94	1.14	12.68
KPT sample	48.50	25.00	0.06	0.50	2.76	1.56	13.15
SSB sample	62.91	25.83	0.25	0.13	5.75	1.68	2.03

Note: [a]Total iron content; [b]Loss on ignition

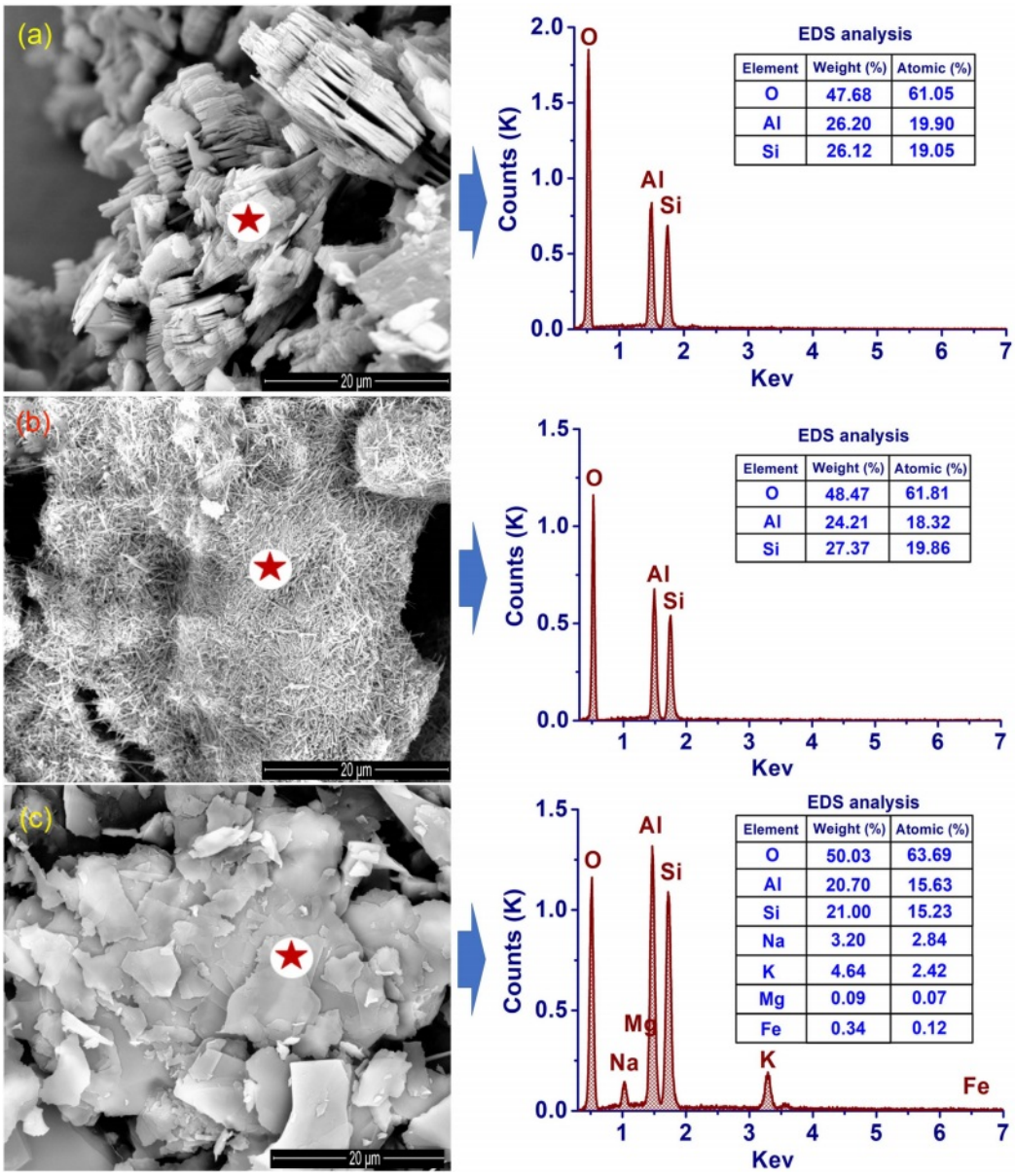

Fig. 2. SEM images and EDS point analysis results of the natural materials. Note: (a) KLC sample; (b) KPT sample, and (c). SSB sample. The star position is the EDS point.

low temperatures (about 100 ºC) are desorption of surface H_2O and dehydration. The formation of the metakaolin phase is indicated by endothermic peaks at 411 °C for the halloysite sample (KPT) and at 436 °C for the kaolinite sample (KLC) [18]. The $SiO_2(\alpha) \rightarrow SiO_2(\beta)$ quartz phase transition in the samples is represented by low-to-high temperature endothermic peaks as follows at 559 °C (KPT), 569 °C (KLC), and 575 °C (SSB) (Fig. 3) [11, 17]. The difference in the temperature of the endothermic peaks between the samples may be due to differences in mineral morphology, composition, and grain size. The KPT sample contains nano-sized tabular halloysite minerals, which may contribute to a decrease in the temperature of the metakaolin and quartz transitions. The SSB sample has the highest temperature of the three samples, indicating platy sericites' natural stability. The TGA analysis in Fig. 3 shows the change of materials in mass during the heating process. Mass deductions are 12.76%, 16.68%, and 3.99% for the KLC, KPT, and SSB samples. This result is consistent with the XRF analysis above, through the loss on ignition value.

Characterization of the mullitization

XRD analysis

Fig. 4 shows the XRD patterns of the KLC, KPT, and SSB samples calcinated at 1000 ºC, 1200 ºC, and 1400 ºC. The XRD patterns of the three materials (KLC10, KPT10, and SSB10) indicate that quartz is the primary phase at 1000 ºC. Other weak phases are amorphous

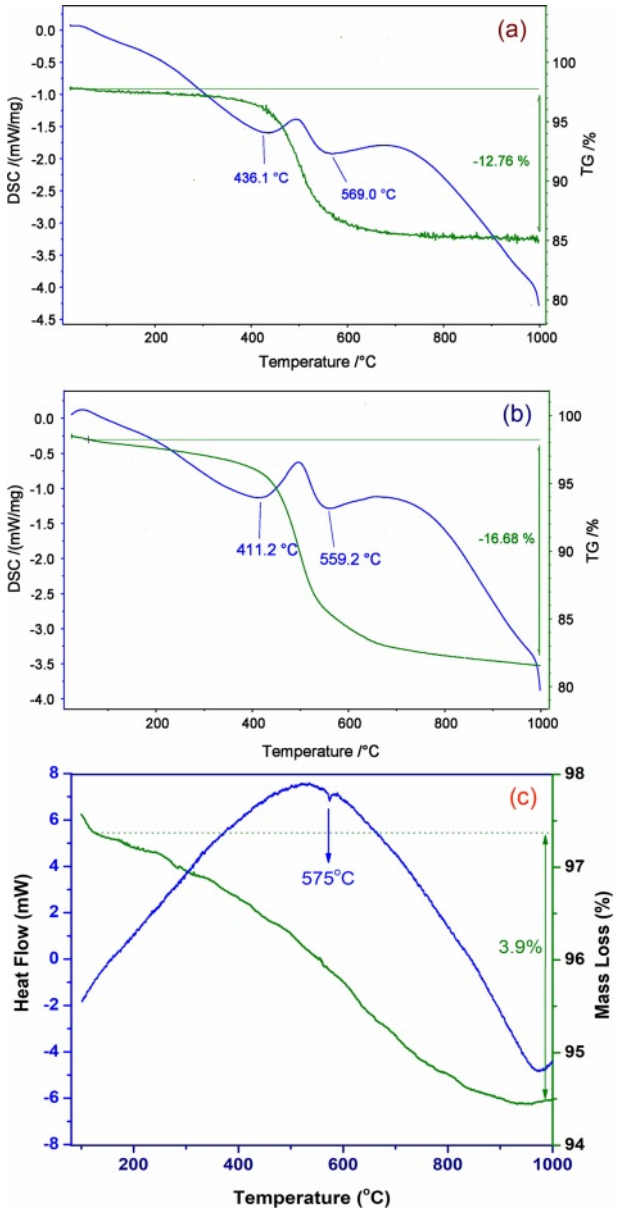

Fig. 3. TG-DSC curves of the KLC (a), KPT (b) samples, and TG-DTA curve of the SSB sample (c).

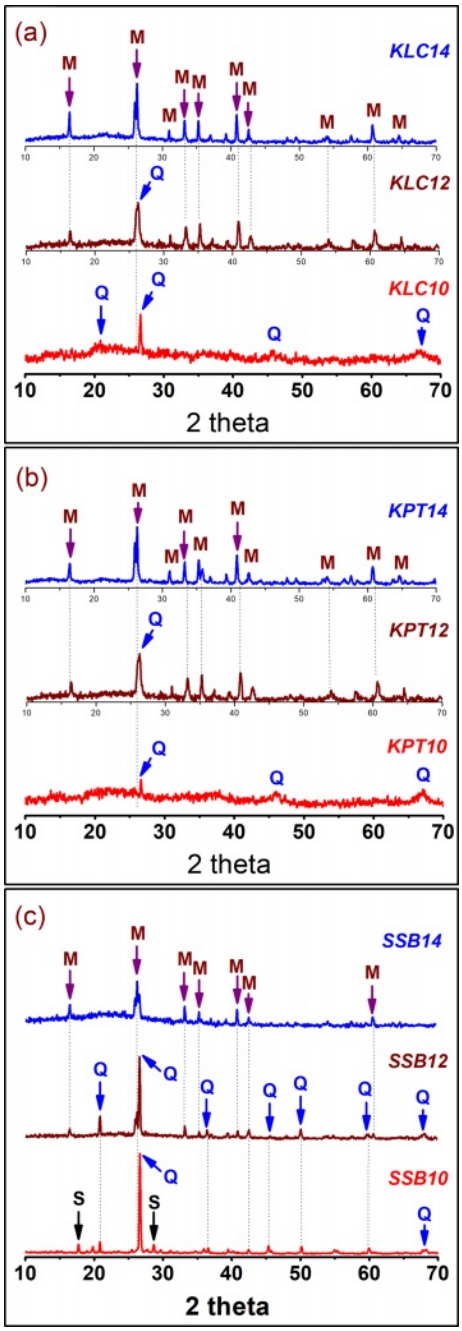

Fig. 4. XRD patterns of the natural samples (KLC, KPT, SSB) at different temperatures (at 1000 ºC (10), 1200 ºC (12), and 1400 ºC (14)), S-sericite, Q-quartz, and M-mullite.

(KLC10, KPT10) and sericite (SSB10). This proves that sericite is more stable than kaolinite and halloysite minerals during heating. After sintered at 1200 ºC, there were two mineral phases, including quartz (Q), and the new mineral mullite (M) emerged in KLC12, KPT12, and SSB12, while the sericite disappeared (SSB12). However, their XRD intensities are low and maybe because this is the early stage of the mullitization phase formation. This process is more substantial and apparent at the calcination temperature of 1400 ºC. Here, the XRD patterns of the materials (KLC14, KPT14, and SSB14) all clearly show the new mineral, mullite; meanwhile, the XRD peaks of quartz gradually disappeared. The results agree with the thermal analysis in other reports for kaolinite, halloysite, and sericite minerals [19, 20].

SEM observation

The phase transformation of initial natural materials (KLC, KPT, and SSB) to mullite and sinterability were also investigated by using SEM. Fig. 5 shows the SEM images of these samples that were calcinated at 1400 ºC. The morphology of the materials in the samples calcined at 1000 ºC has a molten form, exhibiting an amorphous phase (not shown here). Meanwhile, SEM images of pieces at 1400 ºC (KLC14, KPT14, and

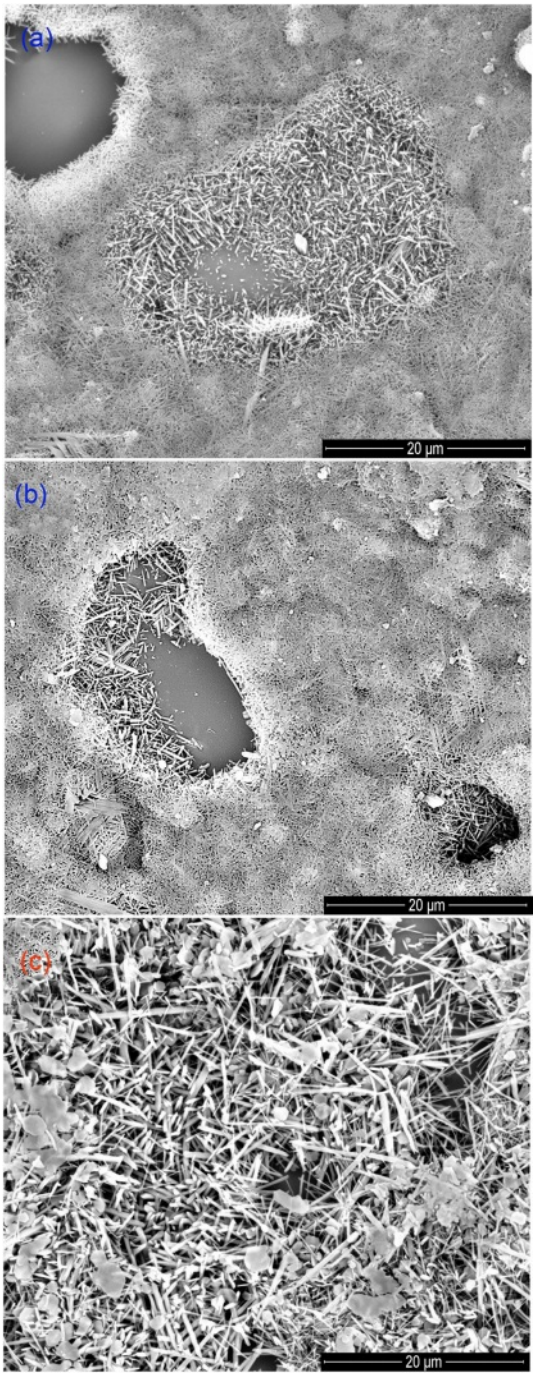

Fig. 5. SEM images of the samples (KLC (a), KPT (b), and SSB (c)) at 1400 ºC.

SSB14) clearly show well-crystallized mullites. The fibrous and rod-shaped mullites were homogeneously distributed and formed with an interlocking network. The mullite density increased when the sintering temperature was raised to 1400 °C. Therefore, the compressive strength of the ceramic body at 1400 ºC can be higher than at 1000 ºC. Fig 5 also shows the different sizes of the mullite crystals in the sample at 1400 ºC. The mullite in the SSB14 is larger than the mullite crystals of KLC14 and KPT14. Thus, the mineral compositions of the starting materials (kaolinite, halloysite, and sericite) and their grain sizes can affect the mullite crystal size and the smoothness of ceramics. In addition to the chemical composition, the mineral composition, morphology, and grain size of starting materials such as pseudo-hexagonal kaolinite, tabular halloysite, and platy sericite can also influence the mullitization process and the size of formed mullite crystals during calcination. These factors can significantly affect the quality of ceramic products and thus require further investigation.

Conclusion

The study employed various characterization techniques, including XRD, XRF, thermal analysis, and SEM-EDS, to investigate the properties of three types of natural materials (KLC, KPT, and SSB) from regular deposits in Vietnam and their mullitization process at different calcination temperatures. The results showed that kaolinite, halloysite, and sericite are the predominant minerals in KLC, KPT, and SSB samples, respectively, under 2 µm particle sizes. These minerals exhibit typical morphologies, including pseudo-hexagonal and stratified kaolinite, tubular halloysite, and thin platy sericite. The primary chemical compositions of the samples are SiO_2 and Al_2O_3, followed by (K_2O+Na_2O), TiO_2, and total iron content. Thermal analysis revealed the three materials exhibited different temperatures for their quartz phase transitions, with low-to-high temperature endothermic peaks occurring at 559 °C (KPT), 569 °C (KLC), and 575 °C (SSB). The metakaolin phase was formed at different temperatures for the halloysite and kaolinite samples, as indicated by endothermic peaks at 411°C for KPT and 436 °C for KLC. To investigate mullitization, the materials were calcinated at 1000 °C, 1200 °C, and 1400 °C for two hours with a heating rate of 10 °C/min. The XRD and SEM analysis results revealed that mullitization began at temperatures above 1000 °C and was prominent at nearly 1400 °C, with well-crystallized mullites appearing. Moreover, the SSB samples displayed larger mullite crystals than those in the KLC and KPT samples when sintered at 1400 °C. The results presented in this study can be important information for producing traditional ceramics or other advanced materials using these natural materials.

Acknowledgments

This research was financially supported by the Hanoi University of Mining and Geology (HUMG) - Vietnam, under grant number T22-25.

References

1. V.J. Silva, E.P. Almeida, W.P. Gonçalves, R.B. Nóbrega, G.A. Neves, H.L. Lira, R.R. Menezes, and L.N.L.

Santana, Ceram. Int. 45[4] (2019) 4692-4699.
2. L. Yuan, B. Ma, Q. Zhu, X. Zhang, H. Zhang, and J. Yu, Ceram. Int. 43[7] (2017) 5478-5483.
3. S. Sutardi, R. Septawendar, and A. Rachman, J. Ceram. Process. Res. 14[3] (2013) 200-404.
4. C.Y. Chen, G.S. Lan, and W.H. Tuan, J. Eur. Ceram. Soc. 20[14] (2000) 2519-2525.
5. M.G.M.U. Ismail, Z. Nakai, K. Minegishi, and S. Sōmiya, Int. J. High Technol. Ceram. 2[2] (1986) 123-134.
6. A.R. Romero, H. Elsayed, and E. Bernardo, J. Am. Ceram. Soc. [101] (2018) 1036-1041.
7. T. Boyraza and A. Akkus, J. Ceram. Process. Res. 22[2] (2021) 226-231.
8. H. Tan, Int. J. Mineral Process. 100[3] (2011) 188-189.
9. Z. Tong, M. Li, D. Li, K. Wu, and X. Yang, J. Ceram. Process. Res. 24[2] (2023) 308-320.
10. V.J. Silva, M.F. Silva, W.P. Gonçalves, R.R. Menezes, G.A. Neves, H.L. Lira, and L.N.L. Santana, Ceram. Int. 42[14] (2016) 15471-15478.
11. L. Yuan, J. Yu, R. Ye, and S. Zhang, J. Ceram. Process. Res. 14[4] (2013) 525-528.
12. N.T.T. Thao, J. Min. Earth Sci. 60[6] (2019) 42-50.
13. N.T.T. Thao and N.X. Thanh, J. Geo. Serie. A 340 (2014) 37-45 (in Vietnamese).
14. P.T. Xuan, N.V. Pho, D.T Tra, H.T. Nga, PT. Dang., N.T. Lien, and N.T.T. Thao, Vietnam J. Earth Sci. 35[2] (2013) 97-106 (in Vietnamese).
15. B.H. Bac and N.T. Dung, 2016, Vietnam J. Earth Sci. 34 (2016) 275-280.
16. S. Hillier and P.C. Ryan, Clay Miner. 37 (2002) 487-496.
17. N.T.T. Thao, J. Geol. Soc. Korea. 59[1] (2023) 159-168.
18. S. Demir and S. Yaşın, J. Ceram. Process. Res. 23[1] (2022) 41-47.
19. X. Wang, J.-H. Li, W.-M. Guan, M.-J. Fu, and L.J. Liu, Mater. Des. 89 (2016) 1041-1047.
20. W. Suthee and W. Darunee, J. Ceram. Process. Res. 20[6] (2019) 643-648.